Atmospheric Environment 79 (2013) 188–197

Contents lists available at SciVerse ScienceDirect

Atmospheric Environment

journal homepage: www.elsevier.com/locate/atmosenv

Emission characteristics and air–surface exchange of gaseous mercury at the largest active landfill in Asia

Wei Zhu [a,e], Zhonggen Li [a,*], Xiaoli Chai [b,*], Yongxia Hao [b], Che-Jen Lin [a,c,d], Jonas Sommar [a], Xinbin Feng [a]

[a] State Key Laboratory of Environmental Geochemistry, Institute of Geochemistry, Chinese Academy of Sciences, Guiyang 550002, China
[b] State Key Laboratory of Pollution Control and Resource Reuse, Tongji University, Shanghai 200092, China
[c] Department of Civil Engineering, Lamar University, Beaumont, TX 77710, USA
[d] College of Environment and Energy, South China University of Technology, Guangzhou 510006, China
[e] University of Chinese Academy of Sciences, Beijing 100049, China

HIGHLIGHTS

- The emission of gaseous elemental mercury from the largest active landfill in Asia is characterized.
- The interstitial gas mercury concentration in the landfill exhibits significant spatial variability.
- Gaseous elemental mercury concentration in landfill gas declines with the age of landfill cells.
- Strong mercury emission from MSW surface can be effectively contained by application of a thin layer clay cover.

ARTICLE INFO

Article history:
Received 7 March 2013
Received in revised form
20 May 2013
Accepted 28 May 2013

Keywords:
Landfill
GEM flux
Landfill gas
Interstitial gas GEM
Shanghai

ABSTRACT

The emission characteristics and air-surface exchange of gaseous elemental mercury (GEM) at Laogang landfill in Shanghai, China, the largest active landfill in Asia, has been investigated during two intensive field campaigns in 2011 and 2012. The mercury (Hg) content in municipal solid waste (MSW) varied widely from 0.19 to 1.68 mg kg^{-1}. Over the closed cell in the landfill, the mean ambient air GEM concentration was virtually indistinguishable from the hemispherical background level (1.5–2.0 ng m^{-3}) while the concentration downwind of ongoing landfill operation (e.g. dumping, burying and compacting of MSW) was clearly elevated. GEM emission through landfill gas (LFG) was identified as a significant source. GEM concentrations in LFGs collected from venting pipes installed in different landfill cells varied widely from 3.0 to 1127.8 ng m^{-3}. The GEM concentrations were found negatively correlated to the age of LFG cells, suggesting GEM released through LFG declined readily with time. The GEM emission from this source alone was estimated to be 1.23–1.73 mg h^{-1}. GEM emission from cover soil surfaces was considerably lower and at a scale comparable to that of background soil surfaces. This is in contrast to earlier reports showing enhanced GEM emissions from landfill surfaces in Southern China, probably due to the difference in soil Hg content and gas permeability characteristics of soils at different sites. Vertical concentration profiles of GEM in the interstitial gas of buried MSW were sampled, perhaps for the first time, which exhibited a wide spatial variability (4.9–713.1 ng m^{-3}) in the 3-year-old landfill cell investigated. GEM emission from landfill operation was estimated to be 290–525 mg h^{-1} using a box model. This suggests that GEM degassing from Laogang landfill is quantitatively largely dominated by emissions from daily landfilling operations with a much smaller contribution from LFG venting and insignificant (bi-directional fluxes near zero) contribution from surfaces capped with a soil layer. This study reveals divergent GEM emission patterns among landfill cells of different ages, and provides essential emission estimates for formulating Hg emission reduction strategies for a large landfill.

1. Introduction

Mercury (Hg) is a ubiquitous persistent pollutant being subject to long-range transport and environmental cycling (Durnford et al., 2010). Concern of Hg pollution is mainly from its potent bio-accumulative

* Corresponding authors. Tel.: +86 851 5890 446; fax: +86 851 5891 609.
E-mail addresses: lizhonggen@vip.skleg.cn (Z. Li), xlchai@tongji.edu.cn (X. Chai), fengxinbin@vip.skleg.cn (X. Feng).

1352-2310/$ – see front matter © 2013 Elsevier Ltd. All rights reserved.
http://dx.doi.org/10.1016/j.atmosenv.2013.05.083

toxicity to human health and wildlife, especially its methylated species are potent neurotoxins (Clarkson and Magos, 2006). Release of Hg into the atmosphere occurs from both natural and anthropogenic sources. Instituting a reliable source inventory for Hg is crucial to better understand its global cycling and environment risk. Recent emission estimates showed that anthropogenic Hg emission sources account for one third of global atmospheric Hg release (Pirrone et al., 2010), and that Asia contributes nearly 50% of the anthropogenic emissions (Lin et al., 2010a; Pacyna et al., 2006; Streets et al., 2009). Hg released from global waste disposal was estimated to be 187 Mg yr^{-1}, approximately 8% of the total anthropogenic emissions. However, the estimate from this sector exhibits large uncertainties due to the lack of field measurement data (Pirrone et al., 2010).

Globally, the primary MSW management alternatives are landfilling, composting, and incineration. Due to its cost-effectiveness and technological simplicity for implementation and maintenance, landfilling has become the most popular method for MSW disposal (Cheng and Hu, 2012). The landfill daily treatment capacity of MSW in mainland China is currently running up to 290×10^3 Mg (Tian et al., 2013). The major Hg containing wastes include batteries, fluorescent lamps, thermometers, medical devices, electronics and electric equipments, whereof batteries and fluorescent lamps contain 54% and 20% respectively of the amount of Hg landfilled in China. Although intensive source reduction efforts have been implemented to reduce Hg content in domestic MSW (Jian et al., 2008) resulting in a rapidly declining trend from 1.8 mg Hg kg^{-1} in 1995 to 0.5 mg Hg kg^{-1} in 2009 (Cheng and Hu, 2012; Hu and Cheng, 2012), the increasing quantities of MSW generated by society constantly add to increment Hg load into landfills.

Hg in MSW landfills may undergo a series of chemical and biological transformation during the lengthy aerobic and anaerobic stabilization processes in the repository, including methylation (Li et al., 2010; Lindberg et al., 2005a), redox chemistry and ligand exchange complexation (Chai et al., 2011a). Eventually, Hg may end up in leachate into groundwater or as volatile species (GEM, $(CH_3)_2Hg$) being released to atmosphere (Baumann et al., 2006; Lindberg and Price, 1999). However, the current knowledge on the long-term fate of Hg in landfills is scarce and largely incomplete. Earlier studies have implied that landfills are an important atmospheric Hg emission source (Feng et al., 2004; Kim et al., 2001; Kim and Kim, 2002; Li et al., 2010; Lindberg and Price, 1999, 2005a, 2005b; Nguyen et al., 2008). Lindberg et al. (2005a; 2005b) observed GEM in LFG up to a μg m^{-3} level for several landfills in Florida, notwithstanding that emission of this species from covered sections of present landfills was unelevated. On the contrary, a survey of several landfills of Southwestern China indicated that volatilization from landfill soil cover represents an important GEM emission source (up to ~1300 ng m^{-2} h^{-1}) and in-turn GEM in LFG vents was present at a considerably lower level (Li et al., 2010).

Shanghai is the largest commercial and industrialized mega-city in China with a population of more than 23 millions. In 2010, approximately 7.32 Tg of MSW was collected in Shanghai, of which 78.4% was landfilled (National Bureau of Statistics, 2011). Shanghai is served by the largest MSW landfill in Asia, Laogang landfill. To better understand the Hg emission from such a large landfill, we performed two intensive field campaigns to quantify air-surface Hg exchange in 2011 and 2012, in order to understand the release of GEM through LFG venting, the spatial distribution in the interstitial gas of landfill cells at different ages and GEM emission from landfill operation.

2. Experimental

2.1. Site description

The Shanghai Laogang MSW Landfill, is at a distance of 75 km southeast of Shanghai City center. Located close to the shore of East China Sea (N 31.054°, E 121.898°, Fig. 1a), it is covering ~6.5 km^2. The landfill was constructed in 1989 and has been operating following four phases (Chai et al., 2011b). The first three phases of disposal cells, equipped solely with passive LFG system, have now been closed. The fourth phase, in operation since late 2005, is a landfill facility equipped with leachate collection system and active landfill gas collection for power generation. The capacity of Laogang phase-4 landfill is 25.57×10^6 m^3 with a daily disposal capability of ~7000 tons. The filling height is about 37 m divided into several vertical sections, each of 7–8 m in height. Generated LFG is actively vented from the top 15 m layer of MSW strata. A 30-cm clay soil layer and a top cover of a high density polyethylene (HDPE) tarpaulin are used for covering the landfill cells. Diurnally, up to 192,000 m^3 of LFG are flared yielding a nominal 10.8 MW power generation capability.

2.2. Sampling and analytical methods

2.2.1. Sampling and analysis of soil and MSW

Surface cover soil and MSW samples were collected for total Hg (HgT) analysis. The clay soil samples were collected from the open area and under the HDPE film cover. The latter were retrieved with the top soil cover removed and HDPE film cut open. All samples were preserved in polyvinyl bags and immediately freeze dried after being shipped to the laboratory. Soil samples were ground and sieved to a 200 mesh using an agate mortar. The MSW samples were ground to a fine powder using a plant blender (JFSD-100, Shanghai Longtuo, China). To avoid cross contamination, the agate mortar and plant blender were thoroughly rinsed with ethanol prior to processing a sample. HgT content in the soil and MSW samples was determined by a Lumex® RA-915 + mercury vapor analyzer coupled with a PYRO 915 + pyrolysis atomizer. Samples were measured in triplicates. A reference standard soil material GSS-5 (Institute of Geophysical and Geochemical Exploration, China) was used as a standard for calibration. The measured average HgT of GSS-5 (287.5 ± 7.0, $n = 6$) compared favourably with the certified value (290 ± 30 μg kg^{-1}).

2.2.2. Measurements of GEM and major components in LFG

Two intensive sampling campaigns were conducted at landfill (December 2011 and September 2012). In the first campaign, samples of GEM and several major gases (CH_4, CO_2, H_2S, and CO) in LFG were collected from a total of 117 venting pipes during first campaign (Fig. 1b) to determine the Hg concentrations at different stages of MSW maturation: 25 venting gas from disposal cells with an age of 6 months, 79 from cells aged 1.5 years, and 13 from the closed phase-3 landfill passive collection system (3 years age). During the second campaign, the youngest cell vents were re-sampled (aged to ca. 1.5 years). The GEM in LFG was monitored using a RA-915+ portable GEM analyzer. Prior to each measurement, the instrument was calibrated using its internal test cell. Six replicate measurements were made for each GEM sample. Remaining above mentioned LFG gas compounds were simultaneously determined using a portable landfill gas monitor (Geotech GA2000 Plus Infrared Gas Analyzer, Geotechnical Instruments-UK). In addition, the LFG temperature was measured by an infrared thermometer.

2.2.3. Measurements of GEM in the interstitial gas of subsurface MSW strata

The distribution of GEM in the interstitial gas of the subsurface MSW strata was determined at different locations on a 3-year-old landfill cell. A gas sampling probe was inserted to different depths (20, 40, 60, and 80 cm) according to a protocol described elsewhere (Chai et al., 2011b). Before sampling, the gas sampling probe was

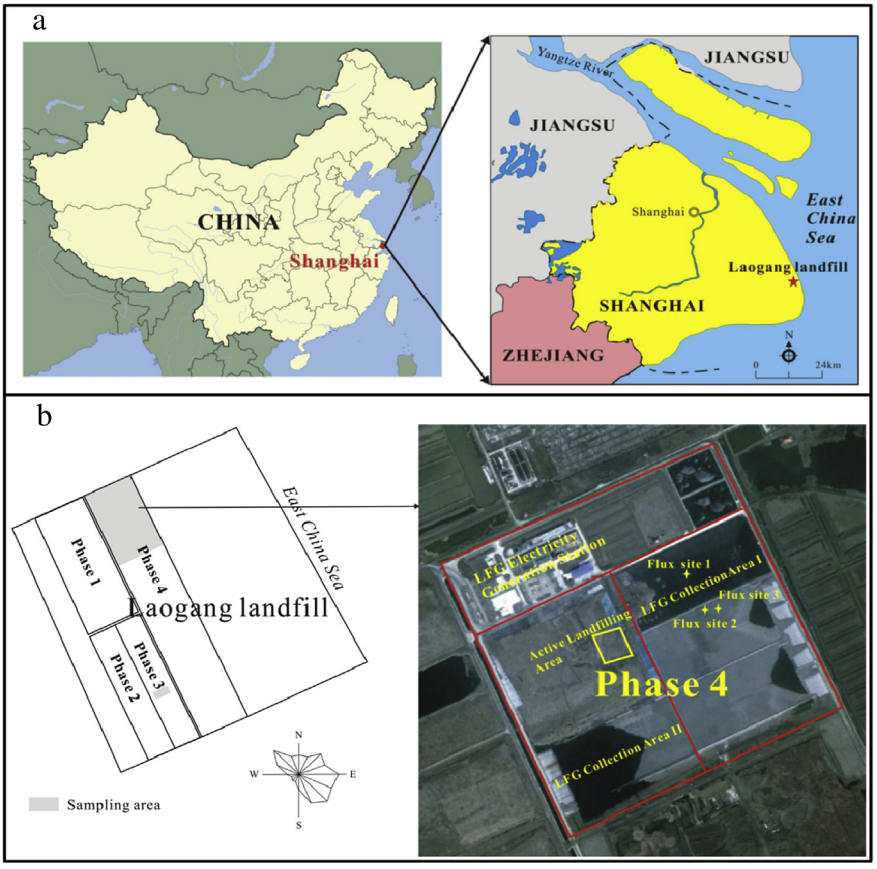

Fig. 1. Sampling Location: (a) location of Shanghai Laogang landfill, (b) schematic view over vent pipe distribution, wind rose for wintertime, and location of GEM flux sampling sites.

allowed for stabilizing at least 30 min. The probe was connected to an automated Hg vapor analyzer (Tekran® 2537B, Tekran Instruments) operated at a reduced sampling flow rate of 0.2 L min^{-1}. Tekran 2537B analyser relies on cold vapor atomic fluorescence spectrometric detection of GEM and utilizes accumulative collection onto gold cartridges in parallel, with alternating operation modes (5-min sampling cycles). A 0.2-μm Teflon membrane filter and a tube filled with dry soda-lime protect the sampling cartridges against contamination by particulate matter and the influence of acidic gases. GEM was measured for four consecutive cycles at each profile depth.

2.2.4. Measurements and estimation of air-surface GEM flux

GEM flux measurements over the top soil cover and MSW surfaces were carried out using a semi-cylindrical shape quartz dynamic flux chamber (DFC) (Fu et al., 2012, 2008; Wang et al., 2005) coupled with an automated Tekran® 2537B Hg vapor analyzer. The DFC was of 10 cm height with a measurement footprint of 0.06 m^2. A 3-way automated magnetic dual switching unit (Tekran® 1110) was utilized to sequentially sample the DFC inlet and outlet air at 10-min intervals (two 5-min samples). This results in a 20-min temporal resolution for calculated air-surface Hg flux. The GEM flux was calculated according to following equation (Xiao et al., 1991):

$$F = \frac{Q(C_o - C_i)}{A} \quad (1)$$

where F is the GEM flux (ng m^{-2} h^{-1}), Q is the DFC internal flushing flow rate (m^3 h^{-1}), A is the footprint (0.06 m^2), C_o and C_i are the GEM concentrations of the DFC outlet and inlet air, respectively. GEM flux measured by DFC method strongly depends on the applied flushing flow rate. A low Q may underestimate Hg flux (Eckley et al., 2010; Lin et al., 2012; Zhang et al., 2002). Therefore, a relatively high flow rate (10 L min^{-1}) was maintained using a diaphragm vacuum pump (DAA-V523-ED, Gast Inc., USA) connected to a gas flow meter (Fu et al., 2008). After the flux measurement, the substrate top layer (down to depth ~2 cm) was sampled for subsequent HgT analysis.

Prior to the field campaign, the DFC was cleaned in the lab by immersion in a 10% HNO_3 (v/v) bath for 24 h followed by repeated rinses in Milli-Q grade water (18.2 MΩ cm). In the field, DFC blanks were consistently low (0.5 ± 0.2 ng m^{-2} h^{-1}, $n = 41$) and not subtracted in Eq. (1). The Tekran® 2537B instruments were systematically calibrated in the laboratory before the field experiments using injections of known amount of Hg^0 from internal and external temperature controlled mercury sources yielding a precision within ±3%. In the field, the instruments were periodically (25–48 h intervals) calibrated by invoking the internal Hg^0 permeation source.

GEM flux measurements were carried out over soil covered MSW surfaces with or without the HDPE film tarpaulin present (Site 1 and 2 respectively, cf. Fig. 1b). To identify the effect of HDPE film cover on landfill surface Hg migration, additional DFC measurement was conducted over bare soil under the shade of a sheet of HDPE film. In addition, flux measurements over bare MSW substrates were conducted at Site 3 (cf. Fig. 1b) and followed-up by a 6-h experiment conducted after application of a 5 cm thick layer of clay soil over the previously investigated plot.

GEM emissions caused by active landfill operation (dumping, burying and compacting) were estimated using a single box model

Table 1
HgT content in the surface soil and MSW samples.

Sample types	Total mercury (HgT, μg kg^{-1})			
	Minimum	Maximum	Mean	Std. dev
Surface soils ($n = 9$)	30	94	52.5	20.4
MSW ($n = 15$)	189	1680	634	428.9

(Lindberg and Price, 1999; Lindberg et al., 2005b) with up- and downwind GEM measurements together with meteorological data as input. The landfill operation area was approximately 100 × 80 m^2. The emitted GEM was approximated to be uniformly dispersed by turbulence throughout the box. The dispersion parameters employed in the model were estimated from *in-situ* meteorological observations (Turner, 1994). Continuous ambient GEM measurement was made using the RA-915 + analyzer operated at 0.2 Hz. To determine the maximum downwind GEM concentration, measurements were made at a series of fixed radii (e.g. 100–150 m) extending from the working face area. In 2011, additional measurements were carried out following a transect parallel to wind direction from up- to downwind of the working area.

2.3. Meteorological data

Meteorological data including solar radiation, wind speed, wind direction, soil moisture, relative humidity, air temperature and soil temperature were collected and stored as 5-min averages using a portable weather station logger (HOBO U-30, Onset Corp., USA). The weather station was set up close to the Hg flux measurement sites with the wind sensors positioned at 2 m above the ground. All time series data in this study are reported in local time (UTC +8 h).

3. Results and discussion

3.1. HgT concentrations in the surface soil and MSW

A summary of HgT content measured in the cover soil and MSW samples is shown in Table 1. The mean HgT content of the soil cover (52.5 μg kg^{-1}) was slightly higher than that (38 μg kg^{-1}) of domestic background soil in China (Feng et al., 2005). HgT content in MSW samples exhibits a significantly higher variability (189–1680 μg kg^{-1}) with a mean of 634 μg kg^{-1} ($n = 15$). In addition, the HgT content in Laogang Phase-4 landfill is significantly lower than that in MSW landfilled at Laogang during the 1990s (1410–5290 μg kg^{-1}, Chai et al., 2011a), a result of stricter policies concerning the application of Hg in house-hold products. For example, Hg usage in battery industry decreases from 582.4 Mg in 1995 to 140 Mg in 2009 (Cheng and Hu, 2012).

3.2. Landfill ambient air GEM concentration

The atmospheric GEM concentrations measured near the landfill surface (10–15 cm) are summarized in Table 2 together with the meteorological data and corresponding GEM fluxes. The GEM concentration level at site 1 was moderate and comparable in magnitude to the hemispherical background (1.5–2.0 ng m^{-3}, Slemr et al., 2011) and in-turn lower than observations previously made in urban Shanghai city air (Friedli et al., 2011). In contrast, GEM in the surface air at site 2 exhibited a comparatively larger variability (1.7–9.2 ng m^{-3}) with a slightly elevated mean concentration of 4.4 ng m^{-3}. However, the enhanced GEM level (13.5–25.2 ng m^{-3}, more details given in Section 3.7) observed 100–200 m downwind of the working face indicated indirectly the GEM degassing from substrates at sites 1 and 2 to be of relative minor magnitude. Fig. 2 illustrates the distribution of ambient GEM as function of wind direction at the two DFC flux sampling sites. At site 1 (~2.5 km from the sea shore), easterly winds originated from the East China Sea were prevailing during the measurements. The winds at site 2 were mainly from west, northwest and north and and the site was thus temporally directly downwind the active landfilling working surfaces at approximately 0.8 km distance (Fig. 1b). The measured atmospheric GEM level at Shanghai Laogang landfill are comparable to those reported for the two landfills in Florida, USA (2.37–40 ng m^{-3}, Lindberg and Price, 1999) and for Nan-Ji-Do landfill in Seoul, Korea (0.73–9.47 ng m^{-3}, Kim et al., 2001), but much lower than those reported for landfills in Guiyang and Wuhan, China (1.6–473.6 ng m^{-3}, Li et al., 2010).

3.3. GEM distribution in LFGs

GEM concentrations in LFGs generated from disposed MSW of different ages, collected by both active and passive venting systems, were measured to understand the GEM migration caused by LFG. Overall, GEM concentrations from 117 LFG venting pipes covered a wide span over 3 orders of magnitude (3.0–1127.8 ng m^{-3}, Fig. 3a). Moreover, for venting pipes of similar ages, there existed a large intra-annual variability of GEM, most likely due to heterogeneity of Hg content in the MSW and other environmental factors (e.g. gas temperature, Kim and Kim, 2002). Statistically, GEM in LFG associated with recently deposited MSW (~6 months old) exhibited a tendency of elevated concentrations (42.2–1127.8 ng m^{-3}) compared to that in the LFG generated by aged MSW (3.0–729.8 ng m^{-3} for the 1.5-year LFG system and 3.0–19.3 ng m^{-3} for the 3-year passive LFG system respectively). In September 2012, LFG of the recent deposited MSW (region II in Fig. 1b) measured during December 2011 was re-sampled. The GEM concentration was found to decrease substantially over this nine month period to 8.8–102.5 ng m^{-3} (Fig. 3a), in spite of the fact that the LFG production rate remained relatively unchanged. In fresh MSW, Hg^0 accounts for a significant fraction of Hg content (more than 80%, Southworth et al., 2005). After landfilled, it is likely that Hg^0 fraction of MSW is attenuated swiftly partitioning to gas streams while the remainder of Hg load interacts strongly with organic and sulfidic materials and remains largely retained within the MSW stratum (Chai et al., 2011a). GEM in the older passive LFG system

Table 2
Statistic summary of the measured air-surface exchange fluxes and ambient concentrations of GEM with the associated meteorological data at three sites at Laogang landfill.

Flux sites	GEM flux (ng m^{-2} h^{-1})				HgT (μg kg^{-1})	GEM concentration (ng m^{-3})			Meteorological parameters			
	Range	Mean	Std	N (emission)		Mean	Std	Range	Solar radiation (W m^{-2})	Air temp (°C)	Air humi (%)	Soil moisture (m^3 m^{-3})
Site 1 (Soil)	−3.7–12.2	3.2	2.7	72(64)	39	1.7	0.12	1.4–2.2	72.4	8.3	91.0	0.341
Site 1 (Shaded)	−3.9–7.6	0.13	2.8	62(29)	39	1.8	0.3	1.3–2.7	0	4.2	85.0	0.332
Site 2 (Soil)	−18.7–22.6	−1.4	10.4	73(37)	43	4.4	2.4	1.8–9.2	111.8	2.8	70.6	0.125
Site 3 (MSW)	4.3–1159.4	216.2	339.5	74(74)	381	4.2	1.1	2.7–6.1	113.5	4.2	72.6	–
Site 3 (5 cm soil)	0.3–34.6	12.6	11.5	17(17)	45	3.1	0.7	2.7–5.2	204.7	8.7	67.5	0.136

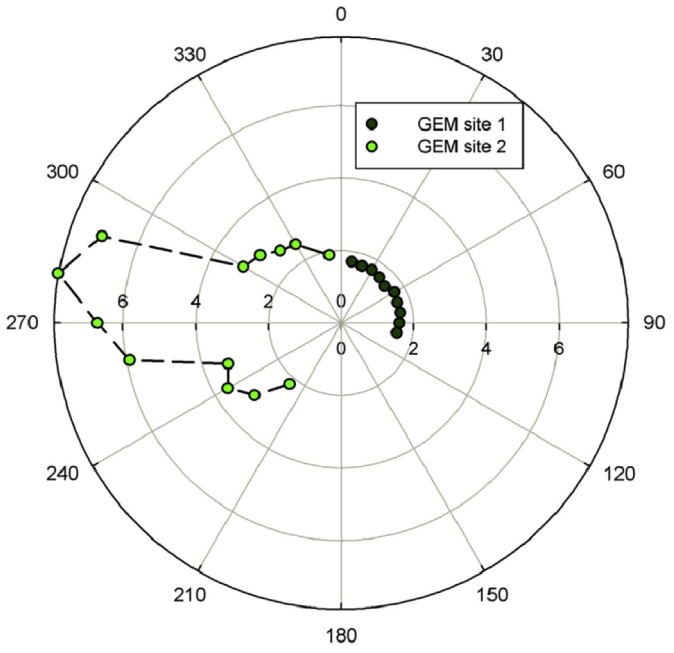

Fig. 2. Wind rose of 20-min averaged surface air GEM distribution during air-soil flux measurements (2 sites).

(Fig. 3a) showed a much narrower concentration range (3.0–19.3 ng m^{-3}), indicating that LFG migration from the closed phases of Laogang landfill is not an important source of GEM.

Fig. 3 displays the distribution of measured gas species in LFG produced from various ages of MSW. Based on the significantly lower HgT content in Laogang landfill MSW compared to that of Gaoyan landfill MSW (HgT range 0.17–46.2 mg kg^{-1}, mean 1.80 mg kg^{-1}; LFG GEM = 2.0–1406 ng m^{-3}, Li et al., 2010), it is to some extent surprising that the GEM level measured in LFG at the two sites is comparable. We suspect that the active LFG collection system at Laogang site has an effect on the GEM volatilization rate from the MSW matrix. The LFG GEM observations in this study are in turn comparable in magnitude to studies elsewhere (de la Rosa et al., 2006; Kim and Kim, 2002) with exception to GEM in LFG of some active landfills in southern Florida (Lindberg et al., 2001; Lindberg and Price, 1999; Lindberg et al., 2005a). Using the data in Fig. 3a together with information of LFG volume flow, we estimate the Hg emissions from the phase-4 active landfill via LFG migration to be in the range 1.23–1.73 mg h^{-1}.

3.4. Relationship between LFG characteristics and GEM concentration

MSW degrades anaerobically to produce CH_4 and CO_2 as the major gases. The observed CH_4 to CO_2 ratio (approximately 3:2 by volume) was stable throughout the campaigns. The mixing ratio of the trace gases (CO and H_2S) did not show significant variation either. Correlations between GEM and other measured gas components of LFG were weak (Table 3). A statistically significant positive correlation was observed between LFG GEM concentration and temperature ($p < 0.01$). As previously reported high temperature may facilitate elevated GEM concentrations in LFG (Kim and Kim, 2002). The GEM-temperature correlation was stronger for the younger disposal cells (~6 months, $r = 0.75$, $p < 0.01$) than for 1.5-year-old cells ($r = 0.48$, $p < 0.01$). CH_4, CO_2, H_2S and CO were weakly or moderately anti-correlated with temperature. The gases essentially produced by anaerobic biological processes making up the bulk of LFG (i.e. CH_4, CO_2, H_2S, CO) and in-turn exhibited weak or moderately negative correlation with temperature. Hence, it may interpret that the release of GEM from buried MSW into LFG is to

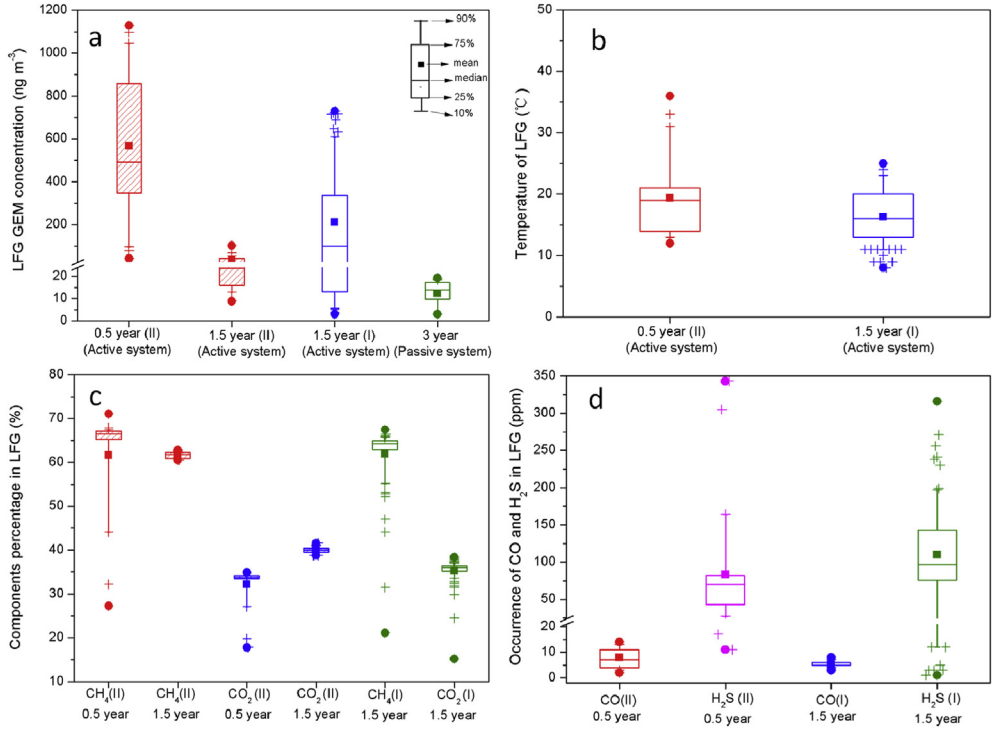

Fig. 3. Box and whiskers percentile plots of GEM, and major gases concentration observations in LFG: (a) GEM in LFG emanating from vents associated with various ages of dumped MSW, (b) LFG temperature, (c) relative proportions (%) of CH_4 and CO_2 and (d) mixing ratios of CO and H_2S in actively pumped vents of two age categories. The (I), (II) represent the sampling area, all the plots from (I) and 0.5 year (II) represent campaign of 2011, 1.5 year (II) from the campaign in 2012.

Table 3
Pearson's correlation matrix between GEM and major LFG gases and gas temperature (significance level indicated as well): (a) 0.5-year filling cell; (b) 1.5-year filling cell.

	GEM	Temp.	CH_4	CO_2	H_2S	CO
a. LFG from vents of 0.5-year old MSW filling cell (II, $N = 25$)						
GEM	1					
Temp.	0.75[a]	1				
CH_4	−0.36	−0.65[a]	1			
CO_2	−0.20	−0.43[b]	0.91[a]	1		
H_2S	−0.27	−0.31	0.06	0.04	1	
CO	0.14	−0.33	0.60[a]	0.55[a]	0.06	1
b. LFG from vents of 1.5-year old MSW filling cells (I, $N = 79$)						
GEM	1					
Temp.	0.48[a]	1				
CH_4	0.23[b]	−0.04	1			
CO_2	0.2	−0.06	0.92[a]	1		
H_2S	0.07	0.08	0.42[a]	0.36[a]	1	
CO	−0.05	0.06	0.06	0.14	−0.20	1

[a] Correlation is significant at the 0.01 level (2-tailed).
[b] Correlation is significant at the 0.05 level (2-tailed).

some extent decoupled from the generation of the biogenic gases. Although both biological and chemical processes have been suggested to cause the release of organic Hg (CH_3Hg^+ and $(CH_3)_2Hg$) in the LFG and in the leachate (Chai et al., 2011a; Lindberg et al., 2005a), the presence of GEM in LFG is likely controlled by physical factors.

3.5. GEM in the interstitial gas of disposed MSW

The vertical profiles of GEM concentration in the interstitial gas of a 3-year-old landfill cell are shown in Fig. 4. To best of our knowledge, this is the first report of GEM measurements in such gas media. Overall, the GEM concentrations ranged from 4.9 to 713.1 ng m^{-3} and exhibited a high spatial disparity, probably due to the inherent heterogeneity of the MSW. There was no obvious dependency with respect to the depth. However, it is apparent that the near-surface concentration (4.9–41.0 ng m^{-3}) was lower compare to that in the deeper strata. At each profile, the GEM concentration at 40-cm depth is moderately higher than that at 20-cm depth. This could induce upward diffusion of pore gas GEM.

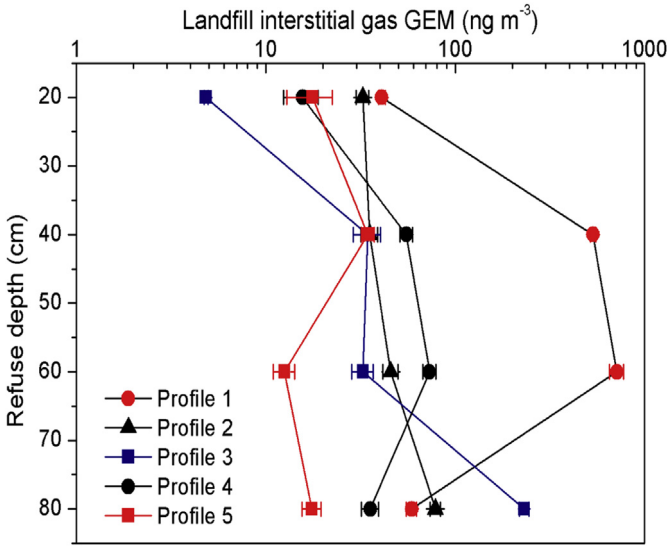

Fig. 4. Vertical profiles of GEM concentration in a 3-year-old landfill cell interstitial gas measured from five locations.

Comparing the GEM profiles in the interstitial gas with the concentrations in the LFG (Fig. 3, 3-year-old passive system), it is found that the GEM in the LFG was present at a lower level ($p < 0.001$). Possible explanations include (1) depletion of Hg^0 in the MSW substrate zone adjacent to LFG wells due to evaporation loss and longitudinal transport, (2) dilution of LFG by intrusion of surface air as the production becomes stagnant, and (3) inorganic divalent Hg in the MSW stabilized by ligand complexation and became less labile to reduction to volatile Hg^0 vapor over time.

3.6. Characteristics of GEM air–surface exchange

3.6.1. GEM exchange flux from landfill top soil cover

Table 2 summarizes the results of GEM flux measurements and concurrent meteorological conditions at the two sampling sites (1 & 2). Overall, the fluxes over soils were bidirectional, in the range of −18.7–22.6 ng m^{-2} h^{-1}. The fluxes were generally of higher magnitude at site 2. Since the final landfilling step is the application of a permanent HDPE film preventing precipitation from entering the landfill cells, the effect of the HDPE sheet on the measured flux was also simulated. A sheet of HDPE tarp was unfurled over the DFC so it was in total shade. In Fig. 5 the evolution of GEM fluxes with and without the HDPE shading is presented. As shown in the Figure, GEM flux likewise exhibits diurnal features over a shaded plot, an observation consistent with earlier reports (Feng et al., 2005; Li et al., 2010; Lin et al., 2012). The maximum flux occurred during midday coinciding with peak solar radiation and temperature (Fig. 5a). With the DFC shaded, the evasive flux was significantly decreased by ~50% but the correlation between soil temperature and Hg flux remained ($r = 0.51$, $p < 0.01$, Fig. 5b). This suggests that soil temperature is a key factor controlling GEM flux from HPDE-covered area. The GEM emission flux from the soil cover is slightly lower than those from natural soil surfaces measured elsewhere in China, including Guangdong China (18.2–135 ng m^{-2} h^{-1}, Fu et al., 2012), Chongqing China (46.5 ± 22.8 ng m^{-2} h^{-1}, Zhu et al., 2011), Guiyang China (0.4–44.4 ng m^{-2} h^{-1}, Feng et al., 2005), Mt. Gongga China (1.5–132 ng m^{-2} h^{-1}, Fu et al., 2008). This is probably due to the lower HgT in the soil (30–94 μg kg^{-1}) compared to those measured in the substrates (60–2000 μg kg^{-1}) of the aforementioned studies.

Figs. 5a and 6 exhibit the diurnal patterns of GEM flux observed during the regular measurements at site 1 and 2 exhibiting emission during daytime and episodes of deposition during nighttime. The mean daytime flux at site 1 was substantially lower than the flux at site 2 under similar meteorological conditions, although the surface soil HgT at both sites was similar (Table 2). A disparity in the soil water content existed between the two sites (near saturation at site 1, 0.341 m^3 m^{-3} and relatively dry at site 2, 0.125 m^3 m^{-3}). Although high water content can accelerate Hg release from soil (Gustin and Stamenkovic, 2005; Kocman and Horvat, 2010; Lin et al., 2010b), water-saturated soil has been reported to restrain GEM transport and therefore reduce evasion (Selvendiran et al., 2008). The considerable deposition flux observed during nighttime at site 2 coincided with an episode of elevated ambient GEM (Fig. 6; $r = -0.82$, $p < 0.001$). Such significant negative correlation was also observed in earlier studies (Xin and Gustin, 2007).

3.6.2. GEM flux over MSW surfaces

Fig. 7a shows the evolution of GEM flux measured over an uncovered MSW surface (site 3) along with selected environmental parameters. The observed flux (4.3–1159.4 ng m^{-2} h^{-1}) compares favourably in magnitude with a previous study conducted in China (Li et al., 2010). Compared to Hg^0 gas exchange measured over natural soils of similar HgT content (Fu et al., 2012; Zhu et al., 2011), fluxes from bare MSW surfaces were 1–2 orders of magnitude

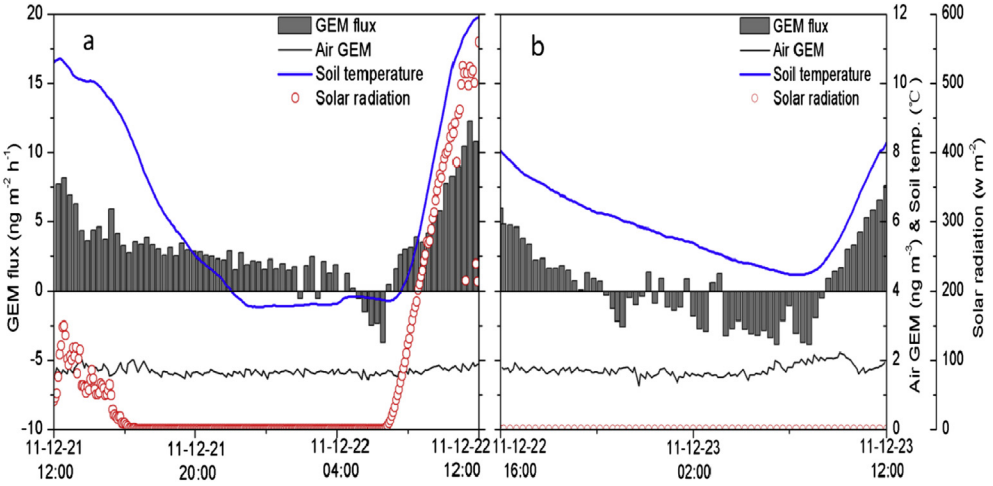

Fig. 5. Time series plot of GEM flux measured over landfill HDPE film covered soil surfaces by open the film: (a) Site 1, (b) Site 1 (Shaded).

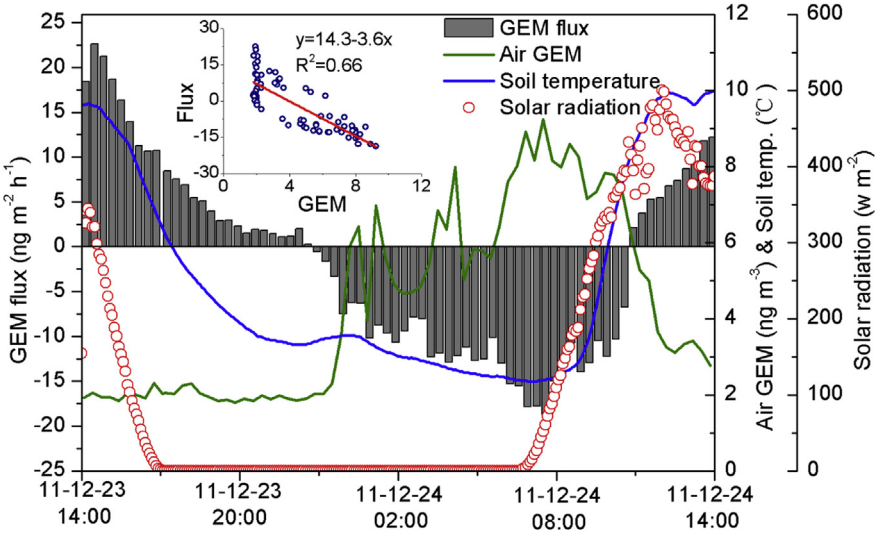

Fig. 6. Time series plot of GEM flux measured over open area soil surfaces. Inlaid is a plot of GEM flux vs. surface air GEM concentration.

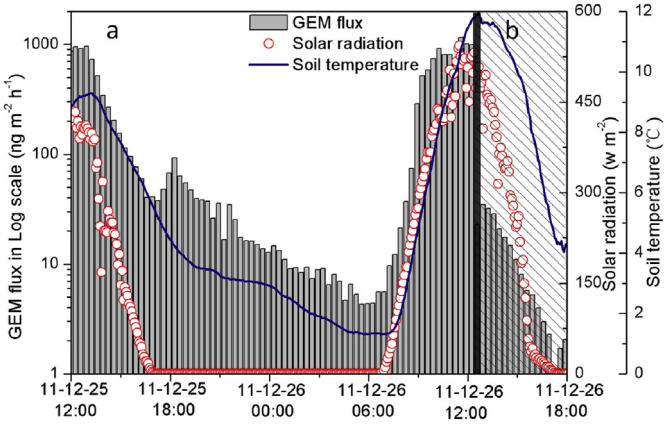

Fig. 7. Time series of GEM emissions flux measured over (a) an uncovered MSW surfaces, and (b) a 5-cm deep soil layer applied over MSW.

higher. This is most likely due to an effect of the Hg speciation in MSW including a pool of Hg^0. Another possibility is that MSW contains a higher fraction of redox-labile Hg compounds. The high correlation observed between solar radiation and GEM fluxes ($r = 0.96$, $p < 0.01$) indicates that rapid light-driven processes (e.g. photoreduction of labile Hg^{II} to Hg^0 followed by volatilization) might have occurred in the surface zone contributing to greater GEM emission. GEM flux was also highly correlated with soil temperature ($r = 0.84$, $p < 0.001$). Using the Arrhenius equation, which relates the emission rate to temperature through E_a, the activation energy of the process (Carpi and Lindberg, 1998; Gustin et al., 2002; Xiao et al., 1991), thermal relationships was evaluated for flux observed under day-light and dark respectively, as:

$$F = Ae^{-E_a/RT} \tag{2}$$

where F is the GEM flux (ng m^{-2} h^{-1}), E_a is the activation energy (kcal mol^{-1}), R is the ideal gas constant (1.9872 cal mol^{-1} K^{-1}), T is the substrate absolute temperature (K), A is a pre-exponential

Table 4
GEM emission from the active landfilling operation estimated using a box model for the five experimental periods.

Sampling time	Downwind (upwind) GEM (ng m^{-3})	Wind speed (m s^{-1})	Pasquill stability*	Distance to working face (m)	Box modeled GEM flux (mg h^{-1})
10:00–11:00 am, Sep. 25, 2012	25.2(2.4)[a]	3.2	B	100	525
15:00–16:00 pm, Sep. 26, 2012	19.0(1.9)[a]	3.5	C	150	430
10:00–11:00 am, Dec. 24, 2011	13.5(1.5)[b]	3.7	C	200	448
15:00–16:00 pm, Dec. 25, 2011	16.5(1.7)[b]	2.1	C	200	310
13:00–14:00 pm, Dec 26, 2011	21.4(1.8)[b]	4.6	D	100	290

*An approach to estimate atmospheric stratification using stability classes denoted by capital letters A–F, where A represents extreme unstable, B unstable etc. (Pasquill, 1961).
[a] Downwind quarter radian average value, the measurement were conducted along a path of fixed radial distance to the working face.
[b] Hour average data, the measurements were conducted at a single sampling site at each of the of up and downwind side of the working face.

factor. Corresponding E_a was estimated to be 151.8 kcal mol^{-1} under sunlight and 116.5 kcal mol^{-1} during nighttime. These values significantly exceed apparent Ea previously estimated from various environmental surfaces: 17.3 ± 7.7 kcal mol^{-1} over background forest soils (Carpi and Lindberg, 1998), 22.0–47.5 kcal mol^{-1} over agricultural soils (Fu et al., 2008), 18.6–69.1 kcal mol^{-1} from urban soil (Feng et al., 2005), and 29.6 ± 1.0 kcal mol^{-1} from the lake water surface (Xiao et al., 1991). In general, the derived E_a values exceed the molar heat of $Hg^0(l)$ vaporization (ΔH^0_{vap}) of 14.7 kcal mol^{-1} (Busey and Giauque, 1953) indicating the Hg^0 emission process from various substrates to be complex and not solely limited by evaporation.

3.6.3. Effect of soil cover on Hg emission

The effect of application of surface clay cover on GEM emission from previously uncovered MSW is shown in Fig. 7b. This experiment was conducted shortly after regular MSW flux measurements during the period of day (12:00– 18:00) when maximum fluxes are expected. A significant suppression of GEM flux was observed with the clay cover. The GEM flux (0.3–34.6 ng m^{-2} h^{-1}) over the 5-cm clay cover was similar to those measured over permanent soil cover. This indicates that the application of a thin clay layer is an effective method to control GEM evasion from MSW. Significant reduction of Hg volatilization can be achieved by a shallow layer of clay soil exhibiting low gas permeability.

3.7. Modeling of Hg emission from the landfill working surface

Using the parameters listed in Table 4, the GEM emission from the active landfill operation was estimated to be 290–525 mg h^{-1}, similar to those found in the landfills in Florida, USA (Lindberg et al., 2005b). It should be noted that the estimated emission range is based on observations recorded during two seasonal periods (autumn and winter) and may not reflect conditions during the warm season. Nevertheless, the GEM concentration 100–200 m downwind of the landfill operation (13.5–25.2 ng m^{-3}) greatly exceeded the background level shown in Table 2 (~1.8 ng m^{-3}), indicating that the landfilling activities were a strong emission source. Consistent with many other landfills in USA and Southwestern China (Li et al., 2010; Lindberg and Price, 1999; Lindberg et al., 2005b), GEM emitted from the working surface is a predominant GEM emission source in landfills.

Table 5 compiles the GEM emissions from different sources in landfills. The relative importance of each category varies significantly between landfills. It is clear that the landfilling operation is the most important source although the emission intensity from

Table 5
Comparison of the GEM emission from landfills in this study with the values reported in the literature.

Location	Surface	Time	Method	Flux (ng m^{-2} h^{-1}) or emission (mg h^{-1})	Substrate HgT (μg g^{-1})	Emission quantity (g yr^{-1})	References (Sumtotal emission: g yr^{-1})
Laogang landfill, Shanghai, China	Covered soil	Dec. 2011	DFC	−18.7–22.6	0.06	222.5	This study (3805.2)
	MSW	Dec. 2011	DFC	4.3–1159.4	0.38	–	
	LFG	Dec. 2011	–	–	–	13	
	Working surface	Dec. 2011, Sep. 2012	Box Model	290–525 mg h^{-1}	0.19–1.68	3569.7	
Gaoyan landfill, Guiyang, China	Covered soil	Nov. 2003, Sep. 2004	DFC	−72.5-1273.3	0.13–1.03	42.0	Li et al., 2010 Feng et al., 2004
	MSW	Nov. 2003, Jan. 2006	DFC	−286.2–5609.6	–	–	(3285.3)
	LFG	2003-2004	–	–	–	0.9	
	Working surface	Sep. 2004	ISCST3 Model	369.0 mg h^{-1}	0.17–46.2	3231.4	
Dazhuanwan landfill, Guiyang, China	Vegetated soil	Mar. 2004	DFC	−65.4–50.9	–	175.9	Li et al., 2010 (184.0)
	Covered soil	Sep. 2004	DFC	−27–3866.5	3.12–6.53	8.1	
JinKou landfill, Wuhan, China	Covered soil	Jun. 2004	DFC	19.6–245.3	–	364.3	Li et al., 2010 (872.4)
	Working surface	Jun. 2004	ISCST3 Model	58.2 mg h^{-1}	0.24–1.27	505.9	
Two landfills in Florida, USA	Covered soil	Apr. 1997	DFC	1–20	0.03–0.15	–	Lindberg and Price, 1999
	Working surface	Apr. 1997	Box Model	5–60 mg h^{-1}	–		(76–110)
Six landfills in Florida, USA	Covered soil	2001–2002	DFC	1–10	–	–	Lindberg et al., 2005
	MSW	2001–2002	DFC	<1–150	–	–	(75–2900)
	Working surface	2001–2002	Box and ISCST3	200–600 mg h^{-1}	–	–	
Nan-Ji-Do landfill, Seoul, S. Korea	Entire surface	Spr, 2000	Aerodynamic	−1164 ± 1276	–	6000	Kim et al., 2001
	LFG	Aut, 2000	–	–	–	23	Kim and Kim, 2002 (6023)
B–C landfill, Dae Gu, S. Korea	Entire surface	Jan. 2004	Aerodynamic	39.0 ± 43.3	–	204.9	Nguyen et al., 2008 (204.9)

different landfills varies greatly. Emissions from closed cells (with top soil cover) and LFG venting in landfills also vary significantly. For instance, from reports of limited number of landfills in Asia, the Hg emission through LFG in Gaoyan landfill in Southwestern China (Li et al., 2010) and Nan-Ji-Do landfill from Korea (Kim and Kim, 2002; Kim et al., 2001) are much smaller than the emission from the landfill cover soil. In contrast, this work and earlier studies at the landfills in Florida, USA show greater Hg emission from LFG than the landfill cover soil. Collectively, landfill gas collection (e.g., active vs. passive), gas production capacity, surface soil characteristic and solid wastes influence GEM emission from LFG venting and over surface cover. Using the results from this study and an earlier report (Li et al., 2010), we estimate that GEM emission the landfills in China is in the range of 150–800 kg yr^{-1}. This value is small compared to grand anthropogenic Hg emission in China, yet the emission may still represent as an important Hg input to local environment.

4. Conclusions and implications

A comprehensive investigation of Hg emission characteristics was performed in Shanghai Laogang landfill, largest in Asia, through the field quantification of Hg concentration and fluxes at different Hg release points. The active landfill operation was found to be the most important source at this site, emitting 290–525 mg h^{-1} of GEM, 3 orders of magnitude higher than the Hg release through LFG (1.23–1.73 mg h^{-1}). The air–surface exchange (−18.7–22.6 ng m^{-2} h^{-1}) over the landfill cover soil yielded a small net emission. In total, the GEM emission from entire active Laogang landfill could be estimate at 292–545 mg h^{-1}. It was also found that GEM release through LFG venting mainly occurs in the early stage of the MSW decomposition process. This is consistent with depletion of volatile Hg content in the MSW over time. A thin layer of clay (with low HgT content and gas permeability) turned out to be effective to suppress GEM volatilization from MSW surfaces. GEM concentrations in the interstitial gas of aged MSW (mean = 105.2 ng m^{-3}) was significantly higher than that in LFG produced from the MSW of similar age (mean = 12.3 ng m^{-3}). The interstitial gas GEM exhibited significant spatial variability (4.9–713.1 ng m^{-3}), probably due to MSW's heterogeneous Hg content and a lack of gas migration in the landfill cells. The emission intensity at Laogang landfill was approximately four times lower than landfills in Southwest China, suggesting the effectiveness of properly managed landfills in reducing Hg emission.

The high GEM emission deriving from the active landfilling operation prompts for sorting out household waste (e.g. removal of fluorescent lamps) prior to landfilling. Actions should also be taken to apply clay cover over a disposal cell as soon as it is practicable. One uncertainty in this study is that it was difficult to obtain a representative distribution of MSW Hg contents throughout the landfill for better assessing the magnitude of changes of Hg emission over the years. In addition, the emission characteristics of Hg from landfills at different regions seem highly variable based on this and earlier studies. This presents a challenge to accurately estimate the Hg emission from landfills at a global scale. The mechanism of Hg release from the disposal cell through LFG needs further research.

Acknowledgements

This research was financially supported by "973" Program (2013CB430003) and the National Science Foundation of China (grants 41030752, 21077103, 51278357, and 51078285). We would like to thank Dr. X. Zhao from Tongji University, Y. Lei from Chongqing Institute of Green and Intelligent Technology, Chinese Academy of Sciences, and the staffs of Shanghai Laogang Waste Disposal Co. Ltd. for assistance with sampling.

References

Baumann, T., Fruhstorfer, P., Klein, T., Niessner, R., 2006. Colloid and heavy metal transport at landfill sites in direct contact with groundwater. Water Research 40, 2776–2786.
Busey, R.H., Giauque, W.F., 1953. The heat capacity of mercury from 15 to 330°K. Thermodynamic properties of solid liquid and gas. Heat of fusion and vaporization. Journal of the American Chemical Society 75, 806–809.
Carpi, A., Lindberg, S.E., 1998. Application of a teflon (TM) dynamic flux chamber for quantifying soil mercury flux: tests and results over background soil. Atmospheric Environment 32, 873–882.
Chai, X.L., Liu, G.X., Wu, J., Tong, H.H., Ji, R., Zhao, Y.C., 2011a. Effects of fulvic substances on the distribution and migration of Hg in landfill leachate. Journal of Environmental Monitoring 13, 1464–1469.
Chai, X.L., Zhao, X., Lou, Z.Y., Shimaoka, T., Nakayama, H., Cao, X.Y., Zhao, Y.C., 2011b. Characteristics of vegetation and its relationship with landfill gas in closed landfill. Biomass & Bioenergy 35, 1295–1301.
Cheng, H.F., Hu, Y.A., 2012. Mercury in municipal solid waste in China and its Control: a Review. Environmental Science & Technology 46, 593–605.
Clarkson, T.W., Magos, L., 2006. The toxicology of mercury and its chemical compounds. Critical Reviews in Toxicology 36, 609–662.
de la Rosa, D.A., Velasco, A., Rosas, A., Volke-Sepulveda, T., 2006. Total gaseous mercury and volatile organic compounds measurements at five municipal solid waste disposal sites surrounding the Mexico City Metropolitan Area. Atmospheric Environment 40, 2079–2088.
Durnford, D., Dastoor, A., Figueras-Nieto, D., Ryjkov, A., 2010. Long range transport of mercury to the Arctic and across Canada. Atmospheric Chemistry and Physics 10, 6063–6086.
Eckley, C.S., Gustin, M., Lin, C.J., Li, X., Miller, M.B., 2010. The influence of dynamic chamber design and operating parameters on calculated surface-to-air mercury fluxes. Atmospheric Environment 44, 194–203.
Feng, X.B., Tang, S.L., Li, Z.G., Wang, S.F., Liang, L., 2004. Landfill is an important atmospheric mercury emission source. Chinese Science Bulletin 49, 2068–2072.
Feng, X.B., Wang, S.F., Qiu, G.A., Hou, Y.M., Tang, S.L., 2005. Total gaseous mercury emissions from soil in Guiyang, Guizhou, China. Journal of Geophysical Research-Atmospheres 110 (D14306). http://dx.doi.org/10.1029/2004JD005643.
Friedli, H.R., Arellano, A.F., Geng, F., Cai, C., Pan, L., 2011. Measurements of atmospheric mercury in Shanghai during September 2009. Atmospheric Chemistry and Physics 11, 3781–3788.
Fu, X.W., Feng, X.B., Zhang, H., Yu, B., Chen, L.G., 2012. Mercury emissions from natural surfaces highly impacted by human activities in Guangzhou province, South China. Atmospheric Environment 54, 185–193.
Fu, X.W., Feng, X.B., Wang, S.F., 2008. Exchange fluxes of Hg between surfaces and atmosphere in the eastern flank of Mount Gongga, Sichuan province, southwestern China. Journal of Geophysical Research-Atmospheres 113 (D20306). http://dx.doi.org/10.1029/2008JD009814.
Gustin, M.S., Biester, H., Kim, C.S., 2002. Investigation of the light-enhanced emission of mercury from naturally enriched substrates. Atmospheric Environment 36, 3241–3254.
Gustin, M.S., Stamenkovic, J., 2005. Effect of watering and soil moisture on mercury emissions from soils. Biogeochemistry 76, 215–232.
Hu, Y., Cheng, H., 2012. Mercury risk from fluorescent lamps in China: Current status and future perspective. Environmental International 44, 141–150.
Jian, X.D., Shen, Y.W., Cao, G.Q., 2008. Investigation of mercury usage in the battery production and recommended reduced countermeasures. Environmental Science and Management 33, 10–13 (in Chinese with abstract in English).
Kim, K.H., Kim, M.Y., 2002. Mercury emissions as landfill gas from a large-scale abandoned landfill site in Seoul. Atmospheric Environment 36, 4919–4928.
Kim, K.H., Kim, M.Y., Lee, G., 2001. The soil–air exchange characteristics of total gaseous mercury from a large-scale municipal landfill area. Atmospheric Environment 35, 3475–3493.
Kocman, D., Horvat, M., 2010. A laboratory based experimental study of mercury emission from contaminated soils in the River Idrijca catchment. Atmospheric Chemistry and Physics 10, 1417–1426.
Li, Z.G., Feng, X., Li, P., Liang, L., Tang, S.L., Wang, S.F., Fu, X.W., Qiu, G.L., Shang, L.H., 2010. Emissions of air-borne mercury from five municipal solid waste landfills in Guiyang and Wuhan, China. Atmospheric Chemistry and Physics 10, 3353–3364.
Lin, C.-J., Zhu, W., Li, X., Feng, X., Sommar, J., Shang, L., 2012. Novel dynamic flux chamber for measuring air–surface exchange of Hgo from soils. Environmental Science & Technology 46, 8910–8920.
Lin, C.-J., Pan, L., Streets, D.G., Shetty, S.K., Jang, C., Feng, X., Chu, H.W., Ho, T.C., 2010a. Estimating mercury emission outflow from East Asia using CMAQ-Hg. Atmospheric Chemistry and Physics 10, 1853–1864.
Lin, C.-J., Gustin, M.S., Singhasuk, P., Eckley, C., Miller, M., 2010b. Empirical models for estimating mercury flux from soils. Environmental Science & Technology 44, 8522–8528.
Lindberg, S., Wallschlaeger, D., Prestbo, E., Bloom, N., Price, J., Reinhart, D., 2001. Methylated mercury species in municipal waste landfill gas sampled in Florida, USA. Atmospheric Environment 35, 4011–4015.

Lindberg, S.E., Price, J.L., 1999. Airborne emissions of mercury from municipal landfill operations: a short-term measurement study in Florida. Journal of the Air & Waste Management Association 49, 520–532.
Lindberg, S.E., Southworth, G., Prestbo, E.M., Wallschlager, D., Bogle, M.A., Price, J., 2005a. Gaseous methyl- and inorganic mercury in landfill gas from landfills in Florida, Minnesota, Delaware, and California. Atmospheric Environment 39, 249–258.
Lindberg, S.E., Southworth, G.R., Bogle, M.A., Blasing, T.J., Owens, J., Roy, K., Zhang, H., Kuiken, T., Price, J., Reinhart, D., Sfeir, H., 2005b. Airborne emissions of mercury from municipal solid waste. I: new measurements from six operating landfills in Florida. Journal of the Air & Waste Management Association 55, 859–869.
National Bureau of Statistics, 2011. China Statistical Yearbook 2011. China Statistics Press, Beijing, China.
Nguyen, H.T., Kim, K.H., Kim, M.Y., Shon, Z.H., 2008. Exchange pattern of gaseous elemental mercury in an active urban landfill facility. Chemosphere 70, 821–832.
Pacyna, E.G., Pacyna, J.M., Steenhuisen, F., Wilson, S., 2006. Global anthropogenic mercury emission inventory for 2000. Atmospheric Environment 40, 4048–4063.
Pasquill, F., 1961. The estimation of the dispersion of windborne material. Meteorological Magazine 90, 33–49.
Pirrone, N., Cinnirella, S., Feng, X., Finkelman, R.B., Friedli, H.R., Leaner, J., Mason, R., Mukherjee, A.B., Stracher, G.B., Streets, D.G., Telmer, K., 2010. Global mercury emissions to the atmosphere from anthropogenic and natural sources. Atmospheric Chemistry and Physics 10, 5951–5964.
Selvendiran, P., Driscoll, C.T., Montesdeoca, M.R., Bushey, J.T., 2008. Inputs, storage, and transport of total and methyl mercury in two temperate forest wetlands. Journal of Geophysical Research-Biogeosciences 113 (G00C01). http://dx.doi.org/10.1029/2008JD000739.
Slemr, F., Brunke, E.G., Ebinghaus, R., Kuss, J., 2011. Worldwide trend of atmospheric mercury since 1995. Atmospheric Chemistry and Physics 11, 4779–4787.
Southworth, G.R., Lindberg, S.E., Bogle, M.A., Zhang, H., Kuiken, T., Price, J., Reinhart, D., Sfeir, H., 2005. Airborne emissions of mercury from municipal solid waste. II: potential losses of airborne mercury before landfill. Journal of the Air & Waste Management Association 55, 870–877.
Streets, D.G., Zhang, Q., Wu, Y., 2009. Projections of global mercury emissions in 2050. Environmental Science & Technology 43, 2983–2988.
Tian, H.Z., Gao, J.J., Hao, J.M., Lu, L., Zhu, C.Y., Qiu, P.P., 2013. Atmospheric pollution problems and control proposals associated with solid waste management in China: a review. Journal of Hazardous Material 252-253, 142–154.
Turner, D.B., 1994. Workbook of Atmospheric Dispersion Estimates, second ed. Lewis Publishers, Boca Raton, pp. 2.2–2.13.
Wang, S.F., Feng, X.B., Qiu, G.L., Wei, Z.Q., Xiao, T.F., 2005. Mercury emission to atmosphere from Lanmuchang Hg-Tl mining area, Southwestern Guizhou, China. Atmospheric Environment 39, 7459–7473.
Xiao, Z.F., Munthe, J., Schroeder, W.H., Lindqvist, O., 1991. Vertical fluxes of volatile mercury over forest soil and lake surfaces in Sweden. Tellus B 43, 267–279.
Xin, M., Gustin, M.S., 2007. Gaseous elemental mercury exchange with low mercury containing soils: investigation of controlling factors. Applied Geochemistry 22, 1451–1466.
Zhang, H., Lindberg, S.E., Barnett, M.O., Vette, A.F., Gustin, M.S., 2002. Dynamic flux chamber measurement of gaseous mercury emission fluxes over soils. Part 1: simulation of gaseous mercury emissions from soils using a two-resistance exchange interface model. Atmospheric Environment 36, 835–846.
Zhu, J.S., Wang, D.Y., Liu, X.A., Zhang, Y.T., 2011. Mercury fluxes from air/surface interfaces in paddy field and dry land. Applied Geochemistry 26, 249–255.